

# Comparative on Electronic Differential Control of In-Wheel Motor Electric Vehicle Based on Sliding Mode Control and Fuzzy Control

Xiao-Bin Fan <sup>\*,\*\*,\*\*\*</sup>, Jie-Wen Li <sup>\*</sup> and Hao Li <sup>\*</sup>

**Keywords :** electric vehicle, electronic differential, sliding mode control, fuzzy control.

## ABSTRACT

The current electronic differential control strategy based on the Ackermann steering model only constrains the speed of the driving wheels and does not consider dynamic performance. This paper is based on wheel hub electric vehicles and focuses on the turning driving conditions of the vehicle. From the perspective of improving the stability of the vehicle's steering control, innovative electronic differential control methods based on sliding mode control and fuzzy control are designed. Taking the vehicle's lateral angular velocity and center of mass side slip angle as control objectives, the vehicle is driven at low speeds through double lane change. The control performance of the two designed electronic differentials is compared and verified with the electronic differential control strategy that evenly distributes the total driving torque. The results indicate that overall, sliding mode control has the best performance, maintaining excellent differential performance under various operating conditions. Based on fuzzy control, there is a certain degree of degradation in electronic differential performance during high-speed driving conditions. The electronic differential control system based on the average distribution of total expected torque can also achieve differential driving of vehicles, but its effect is not as good as the other two.

*Paper Received July, 2024. Revised June, 2025. Accepted June, 2025. Author for Correspondence: Xiao-Bin Fan*

*\* Associate Professor, School of Mechanical and Power Engineering, Henan Polytechnic University, Jiaozuo 454000, P.R. China*

*\*\* Guangxi Key Laboratory of Automobile Components and Vehicle Technology, Guangxi University of Science and Technology, Liuzhou 545006, China*

*\*\*\* Key Laboratory of Road and Traffic Engineering of the Ministry of Education, Tongji University*

*\* Graduate Student, School of Mechanical and Power Engineering, Henan Polytechnic University, Jiaozuo 454000, P.R. China*

## INTRODUCTION

With the common goal of achieving carbon neutrality around the middle of this century, all countries vigorously develop pure electric vehicles (Bai et al., 2021). Among them, the motor and the wheel were integrated to directly provide driving torque in the in-wheel motor electric vehicles, in which the transmission devices such as the differential of traditional fuel vehicles were eliminated (Wang et al., 2020). The electronic differential between the driving wheels has become a key factor affecting the steering stability and driving safety (Tan et al., 2020).

According to the vehicle information, the intention of driver was judged (Yang et al., 2019). The yaw rate, centroid slip angle and other status parameters are taken to be as the control targets, and these actual values was designed to follow the ideal values calculated by the vehicle reference model based on control theories such as sliding mode control and fuzzy control (Zhao et al., 2018). The above is called electronic differential control, by which the differential driving was realized while the stability of the vehicle was improved (Chen et al., 2019).

In reference (Yang et al., 2018), the yaw rate was taken to be as the control target, and a sliding mode controller was designed to follow the ideal value based on the steady-state steering requirements. The results show that the differential coordination of dual in-wheel motor electric vehicle can be well realized by the sliding mode control, which makes the steering performance of the vehicle more superior. On this basis, centroid slip angle was taken to be as the control target together, and sliding mode control was also adopted in reference (Wang et al., 2011). As a result, the centroid slip angle was suppressed within a small range while the electronic differential is realized. In reference (Wu et al., 2017; Wang et al., 2018), an electronic differential control strategy based on fuzzy control was proposed to correct the torque distribution coefficient with the driving wheel slip rate as the control target. The result shows that the torque fluctuation was small, the control effect

was precise, and the electronic differential function can be better realized under the fuzzy control strategy. In reference(Duan et al., 2016), the vehicle speed was taken to be as the control target, and the torque was directly distributed to the driving wheels on both sides based on fuzzy control. As a result, the differential speed of the left and right wheels can be realized under turning conditions, which ensures the driving stability of the electric vehicle under constant and variable speeds. Khan designed a robust differential steering control system (DSCS) for an independent four wheel drive electric vehicle. The proposed DSCS is a combination of forward speed and yaw rate controllers, designed using the robust H<sub>∞</sub> control methodology(Khan et al., 2019).

Hub motors can achieve multiple driving modes and dynamic functions, but their core premise is that the distributed drive control algorithm is excellent enough. Aktas(2020) compared Performance and energy efficiency of induction motors (IM) used in electric vehicle (EV), by applying two control methods, namely the indirect field-oriented control (IFOC) method and the direct torque control (DTC) method. The results indicate that the advantage of DTC over IFOC and the superiority of the proposed sliding mode controller. At present, although the direct torque control strategy for hub motors has fast dynamic response and simple structure, its torque ripple is large, especially in permanent magnet synchronous motors with small moment of inertia.

High performance control of permanent magnet synchronous motors requires obtaining accurate rotor position and related parameters. Anayi presented a new method to estimate the initial rotor position of surface mounted permanent magnet synchronous motor (SM-PMSM) without any form of position or current sensors(Anayi et al., 2020). However, the problem of equation underrank in the online parameter identification process of permanent magnet synchronous motors has not been well solved.

Salari designed a two-stage nonlinear predictive controller. The first stage will reach the appropriate pressure for the brake fluid lines. The second stage, the proper amount of electric regenerative torque is obtained using the electronic braking force distribution (EBD) function and considering all constraints(Salari et al., 2023). However, when designing a controller for the regenerative braking system, it has not yet been possible to effectively consider multiple aspects such as vehicle lateral stability, longitudinal stability, speed tracking characteristics, and regenerative braking energy feedback efficiency.

Due to the fact that the motor is located in a closed hub with a relatively high temperature, thermal protection is particularly important, Ušakovs(2023) designed a double capillary pump unit evaporator LHP (loop heat pipe) for electric

motor. However, when the motor fails, the uneven driving force on the opposite side can easily lead to vehicle yaw instability. Zhang(2015) proposed an active fault-tolerant control (AFTC) system in for electric vehicles with independently driven in-wheel motors (IWMs). The current methods for predicting motor faults usually require a large amount of data on motor usage patterns as support to ensure the accuracy of the prediction, which is difficult to implement. Rolling horizon predictive control is a promising method for development. Lisov(2024) used artificial neural networks to design an electronic differential system for rear wheel drive cars, but the algorithm was only validated on a miniature model car, and more importantly, the prototype car is not all wheel drive. Heredia(2023) proposed a distributed algorithm for active disturbance rejection control based on graph theory principles of multi-agent systems for the electronic differential system of all wheel drive in electric vehicles with four brushless wheel hub motors.

Traditional control methods ignore the coupling relationship between yaw rate and center of mass sideslip angle, and do not consider the energy loss caused by instantaneous motor torque changes in torque distribution and the reduction of vehicle maneuverability. In this paper, sliding mode and fuzzy controllers were designed to solve the yaw moment required in the steering process of the vehicle.

## VEHICLE DYNAMICS MODEL

### Eight-dof vehicle model

From the perspective of vehicle handling stability and safety, through appropriate simplification, an eight-dof vehicle dynamics model was established including vehicle longitudinal motion, lateral motion, yaw motion, roll motion and four wheel rotations, as shown in Fig1.

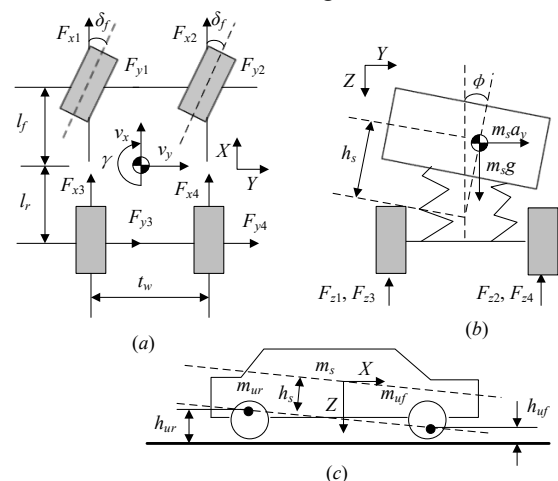


Fig.1 eight-dof vehicle model

It can be seen from the analysis in Fig.1 that during the driving process, the differential equation of longitudinal motion is established as

$$m(\dot{v}_x - v_y\gamma) - m_s(h_g - h_r)\dot{\gamma}\phi = \Sigma F_x - F_{\text{drag}} \quad (1)$$

where  $m$  is the mass of the total vehicle,  $v_x$  and  $v_y$  are the longitudinal and lateral velocity respectively,  $\gamma$  is the yaw rate;  $m_s$  is the sprung mass,  $h_g$  is the height of the center of mass,  $h_r$  is the height of the roll center,  $\phi$  is the roll angle,  $F_{\text{drag}}$  is the sum of the driving resistance, including air resistance, rolling resistance, acceleration resistance and ramp resistance.

Where  $\Sigma F_x$  is the longitudinal resultant force

$$\Sigma F_x = F_{x1} \cos \delta_1 + F_{x2} \cos \delta_2 - (F_{y1} \sin \delta_1 + F_{y2} \sin \delta_2) + F_{x3} + F_{x4} \quad (2)$$

where,  $F_{xi}$  is the longitudinal force of the tire, where  $i=1, 2, 3, 4$ , which refer to the left front wheel, the right front wheel, the left rear wheel and the right rear wheel, respectively.  $\delta_1$  is the wheel angle of the left front wheel and  $\delta_2$  is of the right front wheel.

Differential equation of Lateral motion is as

$$m(\dot{v}_y + v_x\gamma) + m_s(h_g - h_r)\ddot{\phi} = \Sigma F_y \quad (3)$$

where  $\Sigma F_y$  is the lateral resultant force as

$$\Sigma F_y = F_{y1} \cos \delta_1 + F_{y2} \cos \delta_2 + F_{x1} \sin \delta_1 + F_{x2} \sin \delta_2 + F_{y3} + F_{y4} \quad (4)$$

Differential equation of yaw motion is as

$$I_z\dot{\gamma} + I_{xz}\ddot{\phi} = \Sigma M_z \quad (5)$$

where  $I_z$  is the moment of inertia around the Z-axis;  $I_{xz}$  is the inertia product about the X-axis and the Z-axis;  $\Sigma M_z$  is the moment sum around the Z-axis.

$$\Sigma M_z = a(F_{x1} \sin \delta_1 + F_{x2} \sin \delta_2 + F_{y1} \cos \delta_1 + F_{y2} \cos \delta_2) - b(F_{y3} + F_{y4}) + \frac{t_w}{2}(F_{x2} \cos \delta_r - F_{x1} \cos \delta_l + F_{y1} \sin \delta_l - F_{y2} \sin \delta_r + F_{x4} - F_{x3}) \quad (6)$$

where  $a$  is the distance from the center of mass to the front axle,  $b$  is the distance from the center of mass to the rear axle, and  $t_w$  is the wheelbase.

Differential equation of roll motion is as

$$I_x\ddot{\phi} + I_{xz}\dot{\gamma} = \Sigma M_x \quad (7)$$

where  $I_x$  is the moment of inertia around the X-axis;  $\Sigma M_x$  is the moment sum of the vehicle around the X-axis.

$$\Sigma M_x = m_s(h_g - h_r)g\phi - m_s(h_g - h_r)(\dot{v}_y + v_x\gamma) - (K_{\phi f} + K_{\phi r})\phi - (C_{\phi f} + C_{\phi r})\dot{\phi} \quad (8)$$

where  $K_{\phi f}$  and  $K_{\phi r}$  are the roll stiffness of the front and rear suspensions respectively,  $C_{\phi f}$  and  $C_{\phi r}$  are the roll damping of the front and rear suspensions respectively.

The force of the wheel is shown in Fig.2.

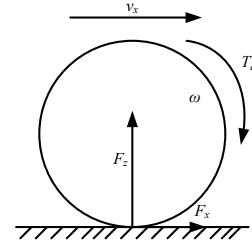


Fig.2 Force diagram of driving wheel

The dual-hub motor electric vehicle with rear-wheel drive and front-wheel steering was as the research object. The two front-steering wheels do not provide driving force for the vehicle, and the output torque of the in-wheel motor  $T_{di}$  is 0. Therefore, the differential equation of the rotational motion of the front wheel is as

$$I_w\dot{\omega}_i = -R_w F_{xi} \quad (9)$$

where  $I_w$  is the moment of inertia of the wheel,  $\omega_i$  is the angular velocity,  $R_w$  is the rolling radius, and  $i=1, 2$ .

The Permanent magnet Brushless DC Motor is integrated into the two rear drive wheels. Therefore, when constructing the dynamic differential equation, the moment of inertia of the in-wheel motor should also be considered as a part of the moment of inertia of the driving wheel. The differential equation is as

$$(I_w + I_m)\dot{\omega}_i = T_{di} - R_w F_{xi} - B_m\omega_i \quad (10)$$

where  $I_m$  is the moment of inertia of the in-wheel motor,  $B_m$  is the motor damping coefficient, and  $i=3, 4$ .

### Two-dof vehicle model

In order to facilitate the study of the changes of the centroid slip angle and yaw rate during the steering process, and to grasp the basic characteristics of its handling stability, the vehicle system was simplified to only the lateral motion along the y-axis and the yaw motion around the z-axis. A linear two-dof vehicle model was obtained, as shown in Fig.3.

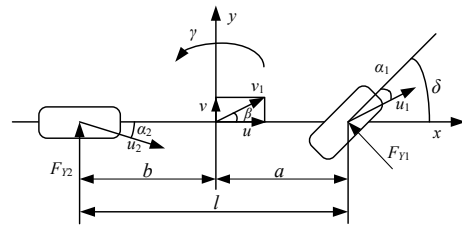


Fig.3 Linear 2-degrees-of-freedom vehicle model

The two-dof reference model is expressed as

$$\begin{cases} m(\dot{v} + u\gamma) = (k_1 + k_2)\beta + \frac{1}{u}(ak_1 - bk_2)\gamma - k_1\delta \\ I_z\dot{\gamma} = (ak_1 - bk_2)\beta + \frac{1}{u}(a^2k_1 + b^2k_2)\gamma - ak_1\delta \end{cases} \quad (11)$$

where  $\delta$  is the front wheel rotation angle,  $u$  and  $v$  are the longitudinal and lateral speeds of the vehicle respectively,  $k_1$  and  $k_2$  are the cornering stiffnesses of the front and rear wheels respectively.

When the vehicle is in steady-state steering,  $\gamma$  and  $\beta$  are approximately constant. Let  $\dot{\gamma} = 0$ ,  $\dot{\beta} = 0$  and the ideal value of yaw rate centroid slip angle can be obtained as

$$\begin{cases} \gamma_d = \frac{u}{l(1 + Ku^2)}\delta \\ \beta_d = \frac{u^2}{l(1 + Ku^2)}\left(\frac{b}{u^2} + \frac{ma}{k_2l}\right)\delta \end{cases} \quad (12)$$

where  $\gamma_d$  and  $\beta_d$  are ideal yaw rate and centroid sideslip angle,  $l$  is wheelbase, and  $K$  represents steady-state yaw rate gain as  $K = \frac{m}{l^2}\left(\frac{a}{k_2} - \frac{b}{k_1}\right)$ .

Considering the road conditions during actual driving, the yaw rate will also be limited as

$$\gamma_u \leq 0.85 \frac{\mu_{peak} g}{u} \quad (13)$$

where  $\mu_{peak}$  is the peak friction coefficient of the road surface.

Therefore, the steady-state ideal yaw rate is as

$$\gamma_d = \min\{|\gamma_d|, |\gamma_u|\} \cdot \text{sgn}(\delta) \quad (14)$$

## CONTROL STRATEGY

While realizing the differential driving of the wheels, the yaw motion characteristics of the vehicle is also taken into account during operation. The overall structure of the control system is shown in Fig.4, which is mainly composed of an eight-dof vehicle model, a linear two-dof vehicle model, an additional yaw moment calculation module and a drive wheel torque distribution module.

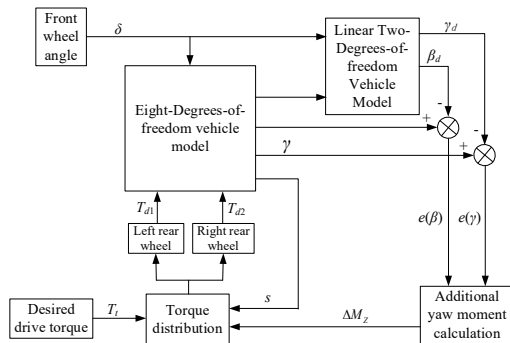


Fig.4 Overall scheme design of electronic differential control system

The specific implementation process is as follows: The linear two-dof vehicle model was used as the reference model of the entire electronic differential control system. According to the input signal of the wheel angle at the current moment, the ideal yaw rate and the centroid slip angle were calculated in real time when the vehicle is in a steady state. The actual value of the yaw rate can be directly obtained by physical sensors such as fiber optic gyroscopes, and the actual value of the center of mass slip angle is calculated by the eight-dof vehicle model. Then the difference between the actual value and the ideal value of the two state variables were taken as input to calculate the additional yaw couple moment required by the vehicle during steering. In the additional yaw moment calculation module, the design of the controller was the core part of the entire electronic differential control system. Based on sliding mode control and fuzzy control, two kinds of controllers were designed to compare and analyze the control effect. The average distribution method is to evenly distribute the total compensation torque required to the four driving wheels.

### Design of sliding mode controller

The sliding mode variable structure control system has strong stability and anti-interference ability, and has good robustness (Mousavinejad et al., 2017). Considering the yaw stability of the vehicle steering, it is necessary to control the driving torque from the left and right rear in-wheel motors, and then adjust the yaw rate and the centroid slip angle to an ideal state. The design block diagram of the electronic differential control system based on sliding mode control is shown in Fig.5.

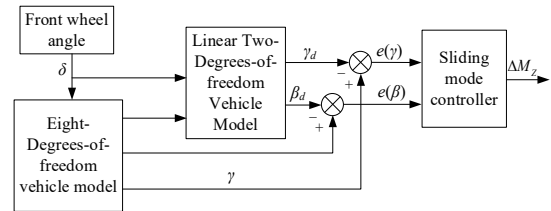


Fig.5 Electronic differential speed strategy based on sliding mode control

The difference between the actual centroid slip angle, the yaw rate and their ideal values were taken as the sliding surface, namely

$$s = \gamma - \gamma_d + c(\beta - \beta_d) \quad (15)$$

where  $c$  is a constant.

Differentiate the sliding surface  $s$ , namely

$$\dot{s} = \dot{\gamma} - \dot{\gamma}_d + c(\dot{\beta} - \dot{\beta}_d) \quad (16)$$

After entering the sliding surface,  $\dot{s} = 0$  was satisfied, namely

$$\dot{s} = \dot{\gamma} - \dot{\gamma}_d + c(\dot{\beta} - \dot{\beta}_d) = 0 \quad (17)$$

Since the front wheel angle input  $\delta$  is very small,  $\delta_1$  and  $\delta_2$  can be considered to be approximately equal, and  $\sin\delta_1$  and  $\sin\delta_2$  can be ignored. Since the research object of this paper was an in-wheel motor electric vehicle with front wheel steering and rear wheel drive, and the two front wheels were driven wheels instead of driving wheels, it can be considered that the longitudinal forces of the two front wheels are equal, namely

$$F_{x1} = F_{x2} \quad (18)$$

Then equations (5) and (6) can be simplified as

$$I_z \dot{\gamma} = a(F_{y1} + F_{y2}) \cos \delta - b(F_{y3} + F_{y4}) + \frac{t_w}{2}(F_{x3} - F_{x4}) \quad (19)$$

where  $M_z = t_w(F_{x3} - F_{x4})/2$ , which is a part of the total required yaw moment  $\Delta M_z$  when the vehicle is under the steering condition.

Equation (19) was simplified as

$$\dot{\gamma} = \frac{1}{I_z} [a(F_{y1} + F_{y2}) \cos \delta - b(F_{y3} + F_{y4}) + \Delta M_z] \quad (20)$$

Equation (20) was substituted into equation (16) as

$$\dot{s} = \frac{1}{I_z} [a(F_{y1} + F_{y2}) \cos \delta - b(F_{y3} + F_{y4}) + \Delta M_z] - \dot{\gamma}_d + c(\dot{\beta} - \dot{\beta}_d) \quad (21)$$

The lateral force on the front and rear axles of the vehicle can also be expressed as

$$\dot{s} = \frac{1}{I_z} \left[ aK_{\varphi f} \left( \delta - \frac{v_y + a\gamma}{v_x} \right) \cos \delta - bK_{\varphi r} \left( \frac{b\gamma - v_y}{v_x} \right) + \Delta M_z \right] - \dot{\gamma}_d + c(\dot{\beta} - \dot{\beta}_d) \quad (22)$$

In order to improve the dynamic quality of the system, the exponential reaching law is used as

$$\dot{s} = -\zeta \operatorname{sgn}(s) - ks, \quad \zeta > 0 \quad k > 0 \quad (23)$$

where  $\zeta$  and  $k$  are constants greater than 0, and they were adjusted by a specific system. By adjusting these two parameters, chattering can be weakened and a good control effect can be obtained.

$\operatorname{Sgn}(s)$  is a symbolic function as

$$\operatorname{sgn}(x) = \begin{cases} -1 & x \leq -1 \\ 0 & -1 < x < 1 \\ 1 & x \geq 1 \end{cases} \quad (24)$$

According to the accessibility condition of the sliding mode, we get

$$s\dot{s} = s(-\zeta \operatorname{sgn}(s) - ks) = -\zeta \frac{s^2}{|s|} - ks^2 \quad (25)$$

where  $\zeta > 0, k > 0$  satisfies the accessibility condition of  $s\dot{s} < 0$ .

According to the Lyapunov function of

$$V(s) = \frac{1}{2} s^2 \quad (26)$$

The derivation was obtained as

$$\dot{V}(s) = s\dot{s} < 0 \quad (27)$$

According to Lyapunov stability theory, the system is stable.

From formula (22) and formula (23), we can

get

$$\frac{1}{I_z} \left[ aK_{\varphi f} \left( \delta - \frac{v_y + a\gamma}{v_x} \right) \cos \delta - bK_{\varphi r} \left( \frac{b\gamma - v_y}{v_x} \right) + \Delta M_z \right] - \dot{\gamma}_d + c(\dot{\beta} - \dot{\beta}_d) = -\zeta \operatorname{sgn}(s) - ks \quad (28)$$

After simplification, the expression of sliding mode controller output  $\Delta M_z$  can be obtained as

$$\begin{aligned} \Delta M_z = I_z & \left[ \dot{\gamma}_d - c(\dot{\beta} - \dot{\beta}_d) - \zeta \operatorname{sgn}(\gamma - \gamma_d + c(\beta - \beta_d)) - k(\gamma - \gamma_d + c(\beta - \beta_d)) \right] \\ & + bK_{\varphi r} \left( \frac{b\gamma - v_y}{v_x} \right) - aK_{\varphi f} \left( \delta - \frac{v_y + a\gamma}{v_x} \right) \cos \delta \end{aligned} \quad (29)$$

In order to reduce chattering, the sigmoid function was used to replace the  $\operatorname{sgn}$  function, where the sigmoid function expression is

$$S = \frac{1}{1 + e^{-x}}$$

By improving the convergence rate of the sigmoid function and designing an exponential term for the sliding surface in the improved convergence rate, the convergence speed of the synchronization error can be accelerated.

### Fuzzy controller design

Fuzzy control is a control based on fuzzy set theory, fuzzy language, and fuzzy logic (Uzunsoy et al., 2018). In order to compare with the sliding mode controller designed above, an additional yaw moment calculation module was designed based on fuzzy control, and the electronic differential control system based on fuzzy control was shown in Fig.6.

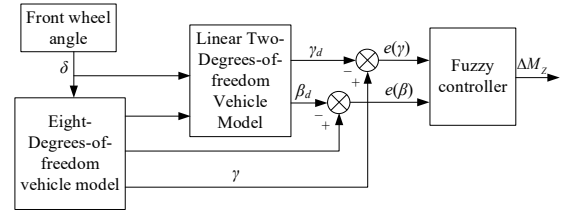


Fig.6 Electronic differential speed strategy based on fuzzy control

The deviations  $e(\gamma)$  and  $e(\beta)$  between the actual yaw rate, centroid slid angle and their ideal values were used as the input of the fuzzy controller, and the output variable was the additional yaw moment  $\Delta M_z$  required for the stable driving of the vehicle. All the three fuzzy universes were  $[-1, 1]$ . The basic domain of  $e(\gamma)$  is  $[-0.05, 0.05]$ , the basic domain of  $e(\beta)$  is  $[-0.005, 0.005]$ , and the basic domain of  $\Delta M_z$  is  $[800, 800]$ .

The membership functions of each linguistic variable were set as trapezoidal and triangular functions. The distribution of each fuzzy subset of  $e(\gamma)$ ,  $e(\beta)$  and  $\Delta M_z$  were shown in Fig.7, Fig.8 and Fig.9.

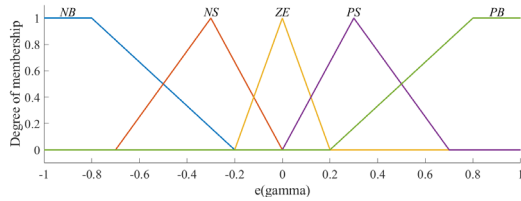


Fig.7 Membership function of  $e(\gamma)$

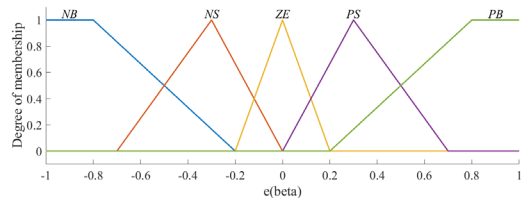


Fig.8 Membership function of  $e(\beta)$

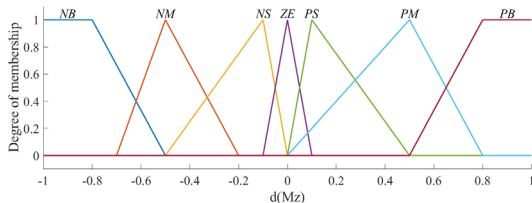


Fig.9 Membership function of  $\Delta M_z$

The fuzzy control rules are shown in Table 1.  
Table 1 Rule table of fuzzy control

$\Delta M_z$	$e(\gamma)$				
	NB	NS	ZE	PS	PB
NB	PB	PB	NS	NB	NB
NS	PB	PM	NS	NM	NB
$e(\beta)$ ZE	PM	PS	ZE	NS	NM
PS	PB	PM	PS	NM	NB
PB	PB	PS	PS	NS	NB

The two deviations of  $e(\gamma)$ ,  $e(\beta)$  were used as inputs. Then the fuzzy controller module with two inputs and one output of the additional yaw moment was built in MATLAB/Simulink. Finally, mamdani inference method was used for fuzzy inference, and the center of gravity method was used to clarify the output PID parameter adjustment.

#### Drive wheel torque distribution based on slip ratio

Drive wheel slip rate was introduced to distribute drive torque to the drive in-wheel motors on both sides. During the steering process, the electronic differential was realized, and the handling stability of the vehicle was further improved. By introducing the torque correction coefficient  $\alpha$ , the corresponding relationship between the correction coefficient and the slip rate of the driving wheel was established, as shown in Fig.10.

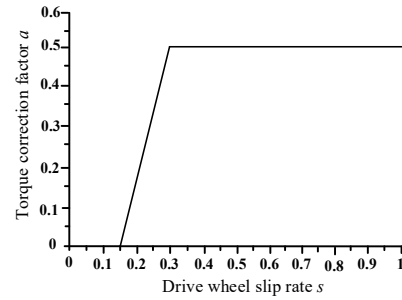


Fig.10 Torque correction factor  $\alpha$  change curve

The mathematical expression of the corresponding relationship between the correction coefficient and the slip rate of the driving wheel is as

$$\alpha = \begin{cases} 0 & 0 \leq s \leq 0.15 \\ \frac{1}{0.3}s - 0.5 & 0.15 < s < 0.3 \\ 0.5 & 0.3 < s < 1 \end{cases} \quad (30)$$

The total demand torque  $T_t$  was obtained through the intention of driver. Combined with the additional yaw moment  $\Delta M_z$  and the torque correction coefficient  $\alpha$ , the target torques of the drive motors on both sides can be calculated as

$$\begin{cases} T_{d12} = T_{d11}(1 - \alpha_1) \\ T_{d22} = T_{d21}(1 - \alpha_2) \end{cases} \quad (31)$$

## SIMULATION ANALYSIS

In order to verify the control effect of the electronic differential control system, the double lane change conditions were respectively set in this paper. The designed electronic differential control system were verified in the simulation cases of low vehicle velocity. Under the condition that the initial velocity and total expected driving torque were set as the same, the total expected drive torque was distributed in three ways, which included differential distribution based on sliding mode control, fuzzy control respectively and average distribution. Finally, the differential effect of the three were compared and analyzed.

#### Simulation parameter setting

Taking the in-wheel motor experimental prototype trial-produced by our research group as the prototype, as shown in Fig.11.

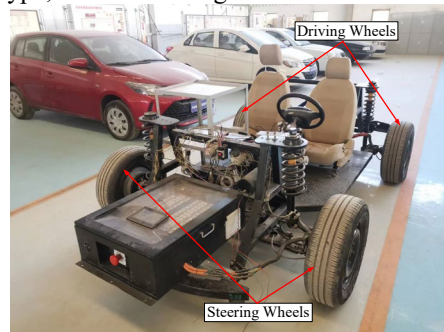
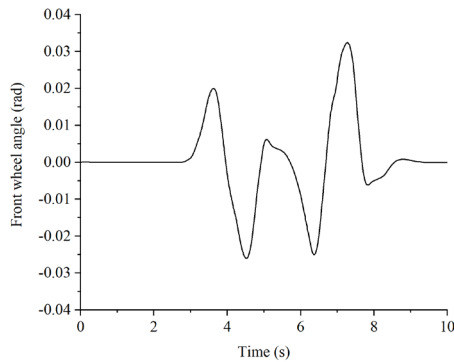


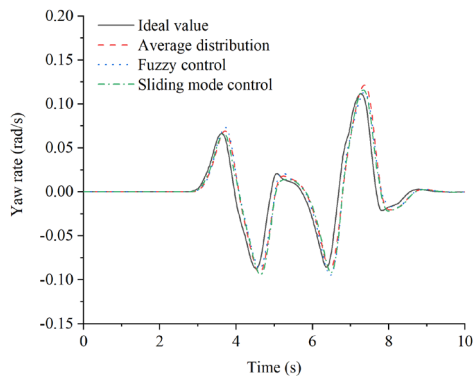
Fig.11 In-wheel motor electric vehicle experimental prototype

**Analysis of simulation results**

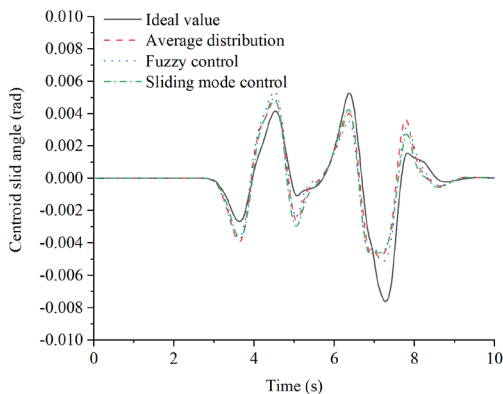
Under the condition of double lane change, the front wheel angle input was shown in Fig.12 (a). The initial velocity of the vehicle was set to 40km/h, the expected total driving torque was 200N·m. The simulation results were shown in Fig.12 (b)~(f). For the convenience of expression, in the following pictures, Average distribution was represented by A, electronic differential based on fuzzy control was represented by F, and electronic differential based on sliding mode control was represented by S.



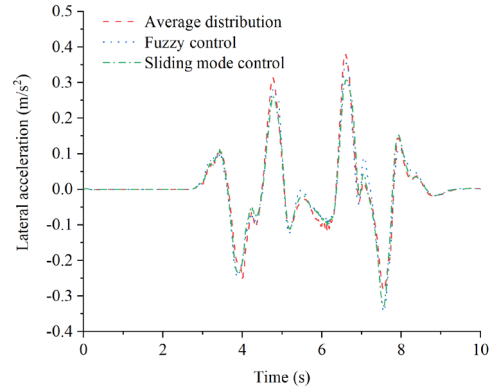
**(a) Front wheel angle**



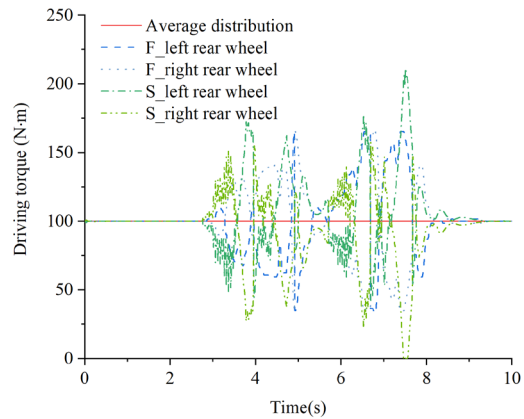
**(b) Yaw rate**



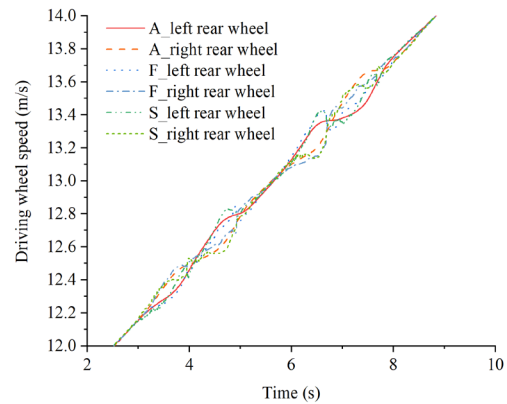
**(c) Centroid slid angle**



**(d) Lateral acceleration**



**(e) Driving torque**



**(f) Driving wheel speed**

Fig.12 Simulation results of 40km/h initial speed with double lane change front wheel angle input

It can be seen from the analysis in Fig.12 (c) that when the vehicle was turning at a low speed, the centroid slip angle was maintained within a small range through any distribution method. When the centroid slip angle of vehicle is small, the handling stability of the vehicle is mainly determined by the yaw rate. Analysis of Fig.12 (b) shows that the ideal value of the yaw rate was best tracked by the electronic differential control scheme based on the sliding mode control on the whole. The electronic differential control scheme based on the fuzzy control

has a slightly worse effect, but its control effect better than the average distribution of the total expected drive torque.

Excessive lateral acceleration may cause the vehicle to slip outside, and even cause the vehicle to roll over in severe cases. It can be seen from the analysis in Fig.12 (d) that the average distribution of the total expected driving torque will cause a large lateral acceleration, which is not conducive to driving safety. Both the electronic differential based on fuzzy control and sliding mode control can effectively reduce the lateral acceleration, and the electronic differential control based on the sliding mode control is better in general.

Analysis of Fig.12 (e) shows that the total desired torque can be differentially distributed by both designed electronic differentials to the driving wheels on both sides according to the wheel angle input. Based on the sliding mode control, the torque distribution value changed more drastically, and the adjustment response to the total expected driving torque was faster according to the real-time vehicle state, which made the control effect more obvious and put forward higher requirements for hardware implementation.

The electronic differential effect can be most directly reflected by wheel speed. It can be seen from Fig.12 (f) that the wheel speed of the left and right driving wheels changed smoothly based on the strategy of drive torque equal distribution, and the differential effect was not obvious. The speed difference between the inner and outer driving wheels of the electronic differential based on the sliding mode control was the most obvious, so the differential effect was the best of these three.

Based on the above analysis, the electronic differential based on the fuzzy control and the sliding mode control can further improve the handling stability while realizing the differential driving in the turning condition, compared with the average distribution. The electronic differential effect based on sliding mode control is better than that of the fuzzy control, and it can better ensure the driving safety.

The comparison of RMSE (Root Mean Squared Error) under double lane change was shown in Table 2. In the table, yaw rate and centroid slid angle are relative to ideal value. Compared to average distribution, sliding mode control improves yaw rate performance by 76.4%, centroid slid angle performance by 68.6%, and lateral acceleration performance by 12.4% under low-speed double lane change conditions. With the great increase of the vehicle velocity, compared with the low-speed double-line shifting front wheel angle input condition, the yaw rate tracking effect of all the three total expected torque distribution methods had become worse. However, in terms of the comparison of these three methods, the electronic differential effect based

on sliding mode control was still better than fuzzy control and average distribution. The centroid slip angle was increased, but also remains within the ideal range. Because the vehicle velocity was greatly increased, the lateral acceleration changed the most, and the three electronic differential control strategies had no obvious control effect in terms of lateral acceleration. For the driving torque distribution problem based on fuzzy control and sliding mode control, the differential amount of total desired torque was increased in general. Especially for electronic differential control strategy based on the fuzzy control, the differential distribution was more obvious than that of low-speed in the second half of the working condition, which also leads to a greater difference in driving wheel speeds.

Table 2 Comparison of RMSE (Root Mean Squared Error) under double lane change

	average	fuzzy	sliding mode
Yaw rate (rad/s)	0.0679	0.0717	0.0160
Centroid slid angle (rad)	0.0035	0.0038	0.0011
Lateral acceleration (m/s <sup>2</sup> )	0.1159	0.1153	0.1015

## CONCLUSIONS

(1) The two electronic differential control systems designed in this paper can both track the ideal centroid slip angle and yaw rate. While realizing the differential driving, the handling stability of the vehicle was improved and the driving safety of the vehicle was ensured.

(2) The designed electronic differential control system based on the sliding mode control has the best effect, and can maintain excellent differential performance under various working conditions. The designed electronic differential control system based on fuzzy control has a certain attenuation of electronic differential performance in high-speed driving conditions. The electronic differential control system based on the average distribution of the total expected torque can also realize the differential driving, but its differential effect is not as good as the other two.

## ACKNOWLEDGMENT

This research was supported by the Key Laboratory of Road and Traffic Engineering of the Ministry of Education, Tongji University (K202303), the Open Project of Guangxi Key Laboratory of Automobile Components and Vehicle Technology (No.2022GKLACVTKF10), College Students' Innovation and Entrepreneurship Training Program (202410460027).

## REFERENCES

- Aktas M., Awaili K., Ehsani M., Arisoy A., "Direct torque control versus indirect field-oriented control of induction motors for electric vehicle applications," *Engineering Science and Technology, an International Journal*, Vol.23, No.5, pp.1134-1143(2020).
- Anayi J., Ibraheemi M., "Estimation of rotor position for permanent magnet synchronous motor at standstill using sensorless voltage control scheme," *IEEE/ASME Transactions on Mechatronics*, Vol.25, pp.1612-1621(2020).
- Bai M., Zhang M., Wang X., "Development policies and trends of global new energy vehicle industry under the background of carbon neutrality," *Information Technology & Standardization*, Vol. 12, pp.13-20(2021).
- Chen X., Liu P., Yang M., Sun L., Luo L. "Electronic differential control strategy for four-wheel wheel drive vehicle based on slip ratio," *Journal of Chongqing University of Technology*, Vol.33, No.3, pp.51-58(2019).
- Duan M., Sun M., Yan P., Lu D., Zhou Z., "Research on electronic differential controller of rear wheel in-wheel motor drive electric vehicle," *Journal of Liaoning University of Technology*, Vol.36, No.3, pp.184-190 (2016).
- Heredia O., Flores O., Cardenas G., Valderrama, J., "Electronic Differential Speed Control for a Four In-Wheel Motors EV Based on a Multi-Agent System," 2023 International Symposium on Electromobility (ISEM), Monterrey, Mexico, pp.1-7(2023).
- Khan A., Aftab F., Ahmed E., Youn I., "Robust differential steering control system for an independent four wheel drive electric vehicle," *International Journal of Automotive Technology*, Vol.20, pp.87-97(2019).
- Lisov A., Panishev S., Gundarev K., "Development of an Electronic Differential System Based on Artificial Neural Networks for Electric Transport," 2024 International Ural Conference on Electrical Power Engineering (UralCon), Magnitogorsk, Russian Federation, pp. 192-196(2024).
- Mousavinejad E., Han L., Yang F., Zhu Y., "Integrated control of ground vehicles dynamics via advanced terminal sliding mode control," *Vehicle System Dynamics*, Vol.55, No.2, 268-294(2017).
- Salari H., Mirzaeinejad H., Mahani F., "A new control algorithm of regenerative braking management for energy efficiency and safety enhancement of electric vehicles," *Energy Conversion and Management*, Vol.276, pp. 116564(2023).
- Tan D., Ge G., Shi L., Yang K., "Research status of electronic differential control of electric vehicle driven by in-wheel motor," *International Journal of Vehicle Safety*, Vol.11, No.4, pp.289-303(2020).
- Ušakovs I., Mishkinis D., Galkin A., Bubovich A., Podgornovs A. "Experimental thermal characterization of the in-wheel electric motor with loop heat pipe thermal management system," *Case Studies in Thermal Engineering*, Vol.47, pp.1-15(2023).
- Uzunsoy E., "A brief review on fuzzy logic used in vehicle dynamics control," *Journal of Innovative Science and Engineering*, Vol2, No.1, pp.1-7(2018).
- Wang P., Tao X., Cao X., "An overview of electronic differential system for pure electric vehicles," *Automobile Applied Technology*, Vol.6, pp.27-30(2020).
- Wang Q., Wang Y., Song X. Investigation into electronic differential strategies based on differential driving[J]. *Journal of Mechanical & Electrical Engineering*, 2011, 28(6): 698-703.
- Wang Y., Yan S., Lu B., Yang J., Zhou H., Liu Z., "Simulation on multifunction steering system of wheel drive electric vehicle," *Journal of Mechanical & Electrical Engineering*, Vol.35, No.10, pp.1128-1132(2018).
- Wu D., Yang L., Jin Y., "The design of electronic differential system based on two times torque distribution," *Automobile Technology*, No.2, pp.51-56(2017).
- Yang P., Zhang H., Sun H., Zhang G., Han X., "A modeling and analysis method for differential control of electric vehicles," *Mechanical Science and Technology for Aerospace Engineering*, Vol.38, pp.870-876(2019).
- Yang Y., Zhao H., Wang W., Xu X., "Study on electronic differential control of electric vehicle with dual in-wheel-motor drive," *Tractor & Farm Transporter*, Vol.45, No.5, pp.34-39(2018).
- Zhang G., Zhang H., Huang X., Wang J., Yu H., Graaf R., "Active fault-tolerant control for electric vehicles with independently driven rear in-wheel motors against certain actuator faults," *IEEE Transactions on Control Systems Technology*, Vol.24, No.5, pp.1557-1572(2015).
- Zhao X., Yu Q., Yu M., Tang Z., "Research on an equal power allocation electronic differential system for electric vehicle with dual-wheeled-motor front drive based on a wavelet controller," *Advances in Mechanical Engineering*, Vol.10, No.2, pp.1-24(2018).